Absolute Configuration and Biological Properties of Enantiomers of CFTR Inhibitor BPO-27

David S. Snyder,[†,‡] Lukmanee Tradtrantip,[†] Sailaja Battula,[†] Chenjuan Yao,[†] Puay-wah Phuan,[†] James C. Fettinger,[‡] Mark J. Kurth,[‡] and A. S. Verkman*,[†]

[†]Departments of Medicine and Physiology, University of California, San Francisco, California 94143-0521, United States
[‡]Department of Chemistry, University of California, Davis, California 95616, United States

S *Supporting Information*

ABSTRACT: We previously reported benzopyrimido-pyrrolo-oxazine-dione (BPO) inhibitors of the cystic fibrosis transmembrane conductance regulator (CFTR) chloride channel and showed their efficacy in a model of polycystic kidney disease. Here, we separated the enantiomers of lead compound BPO-27 (**1**), which contains a single chiral center, and determined their absolute configuration, activity, and metabolic stability. Following separation by chiral supercritical fluid chromatography, the *R* enantiomer, as determined by X-ray crystallography, inhibited CFTR chloride conductance with $IC_{50} \approx 4$ nM, while *S* enantiomer was inactive.

In vitro metabolic stability in hepatic microsomes showed both enantiomers as stable, with <5% metabolism in 4 h. Following bolus interperitoneal administration in mice, serum (*R*)-**1** decayed with $t_{1/2} \approx 1.6$ h and gave sustained therapeutic concentrations in kidney.

KEYWORDS: *Cystic fibrosis, polycystic kidney disease, secretory diarrhea, crystallography*
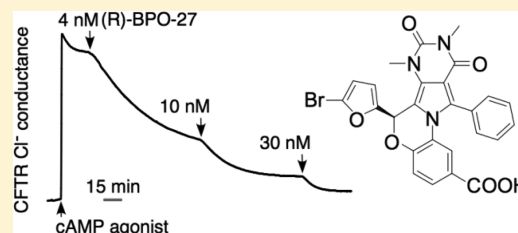
The cystic fibrosis transmembrane conductance regulator (CFTR) protein is a cAMP-regulated chloride channel expressed in secretory and absorptive epithelia.[1] Loss of function mutations in CFTR cause the genetic disease cystic fibrosis (CF). Excess activation of CFTR in intestinal enterocytes occurs in secretory diarrheas that are caused by bacterial enterotoxins, such as cholera.[2,3] CFTR is also involved in fluid secretion into cysts in autosomal dominant polycystic kidney disease (ADPKD).[4,5] CFTR is thus an important drug target, with CFTR activators (potentiators and correctors) for cystic fibrosis therapy and CFTR inhibitors for therapy of secretory diarrheas and ADPKD,[6] and for CF research.

We previously identified several classes of small-molecule CFTR inhibitors, including thiazolidinones (e.g., CFTR$_{inh}$-172),[5,7−9] glycine hydrazides (e.g., GlyH-101),[10−14] and pyrimido-pyrrolo-quinoxalinediones (e.g., PPQ-102),[15] and showed their efficacy in models of polycystic kidney disease and cholera toxin-induced secretory diarrhea. We recently reported an analogue of PPQ-102, the benzopyrimido-pyrrolo-oxazinedione BPO-27 (**1**) (Scheme 1),[16] which inhibited CFTR with $IC_{50} \approx 8$ nM and had greatly improved in vitro metabolic stability and aqueous solubility compared to PPQ-102.[15] Compound **1**, which was synthesized and tested as a racemic mixture (*R/S* 50:50), prevented and reversed renal cyst formation in an embryonic kidney culture model of ADPKD.[16]

We separated **1** into its enantiomers with ≥98.6% enantiomeric excess (e.e.), determined their absolute configuration by X-ray crystallography, and measured their CFTR inhibition activity, metabolic stability, and in vivo pharmacology in mice. A single enantiomer of **1** strongly inhibited CFTR

chloride conductance with $IC_{50} \approx 4$ nM, while the other enantiomer was inactive.

Separation of ~1.0 g racemic (±)-**1** was carried out utilizing chiral supercritical fluid chromatography (SFC) on a RegisCell 3.0 × 25.0 cm column using a combination of CO_2 and ethanol containing 1% 2-propylamine. Two distinct peaks were detected at 230 nm following elution (Figure 1A). Fraction 1 contained 413 mg with 99.5% e.e. (Figure 1B), and fraction 2 contained 396 mg with 98.6% e.e. (Figure 1C). As a consequence of the separation process, the isolated material was not the acid **1**, but the 2-proplyamine carboxylic salt **2**. Optical rotation measurements revealed fraction 1 to be (+)-**2** and fraction 2 to be (−)-**2**. When dissolved in aqueous buffer under physiological conditions, both **2** and **1** convert to the same carboxylate salt form.

CFTR inhibition potency was measured by short-circuit current analysis in FRT epithelial cells expressing human CFTR in the presence of a transepithelial chloride gradient and in which the basolateral membrane was permeabilized with amphotericin B. Under these conditions, short-circuit current is proportional to CFTR chloride conductance. Figure 2A shows no significant inhibition by (−)-**2** at 100 nM, whereas (+)-**2** at 100 nM completely inhibited current. Figure 2B shows the (+)-**2** concentration-dependence, giving an $IC_{50} \approx 4$ nM, as compared to ~8 nM for (±)-**1** as reported previously.[16]

Scheme 1. Transformations of BPO-27[a]

$(\pm)$-**1** (BPO-27) $(-)$-**2** (99.5% e.e.) (S)-**3**

+ enantiomer $(+)$-**2**
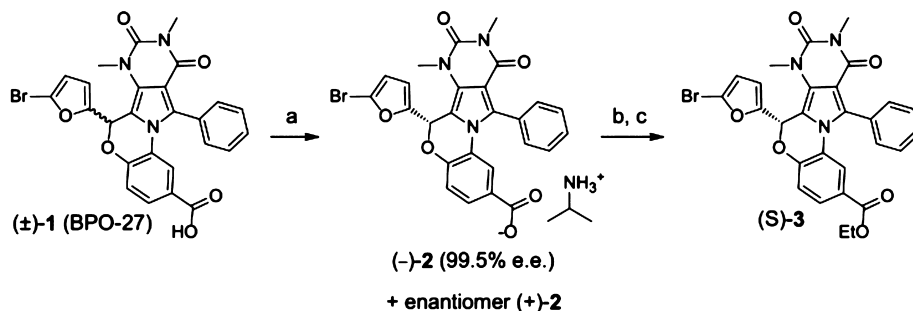
[a]Reagents and conditions: (a) RegisCell 4.6 × 100 mm chiral column, 75% CO_2, 25% EtOH, 0.1% 2-propylamine, 4 mL/min, 100 bar, 25 °C, yield 73%; (b) (i) HCl, H_2O, EtOAc 3× extraction 89% yield; (c) (i) CH_2Cl_2, EDC, DMAP, EtOH, 24 h, (ii) aq. HCl H_2O, 2× extraction, (iii) SiO_2 flash column (2:3 EtOAc/hexane), yield 79%.
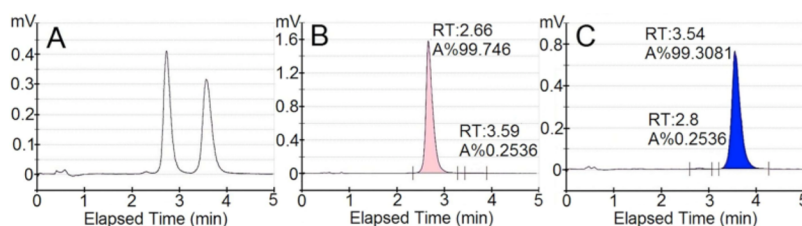

Figure 1. Chromatograms of purified BPO-27 enantiomers following chiral HPLC separation. (A) Analytical chromatogram following preparative separation of ~1 g $(\pm)$-**1**. (B) Chromatogram of fraction 1. (C) Chromatograph of fraction 2, showing retention time (RT) and % area (A%).
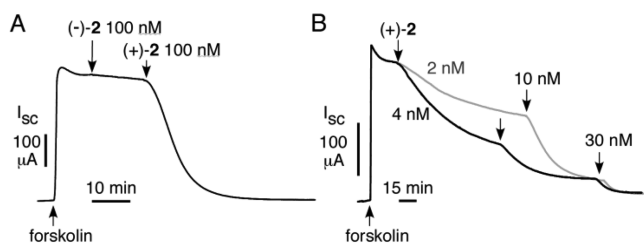

Figure 2. CFTR inhibition by enantiopure $(+)$-**2** and $(-)$-**2**. Short-circuit current was measured in FRT cells expressing human wild-type CFTR in the presence of a transepithelial chloride gradient and following permeabilization of the basolateral membrane. CFTR chloride conductance was activated by 10 μM forskolin. (A) $(-)$-**2** and then $(+)$-**2** (each 100 nM) were added where indicated. (B) $(+)$-**2** added at indicated concentrations, deduced $IC_{50} \approx 4$ nM.

Figure 3. ORTEP representation of the crystal structure of (S)-**3**.

The absolute configuration of the inactive enantiomer was determined by X-ray crystallography. Attempts to crystallize $(-)$-**2** failed to yield X-ray quality crystals, as did the corresponding carboxylic acid **1**, which was isolated by aqueous acidification and organic extraction (Scheme 1, step b). We found that the ethyl ester **3** dissolved in multiple solvents and readily formed large crystals. Chiral ester **3** was thus prepared from inactive $(-)$-**2** (Scheme 1).

X-ray quality crystals of **3** were obtained by vapor diffusion crystallization in toluene and hexane. X-ray analysis revealed the absolute structure to be (S)-**3** (Figure 3); therefore, the active enantiomer has the R configuration. Bioassay of the remaining (S)-**3** crystals confirmed no CFTR inhibition activity at 100 nM, whereas racemic **3** strongly inhibited CFTR.[16]

Although enantiopure $(-)$-**2** was exposed to both acid and base conditions during its purification and conversion to (S)-**3**, racemization did not occur to any significant extent, as it would not have been possible to generate chiral crystals from racemized **3**. The absence of activity of the prepared (S)-**3**
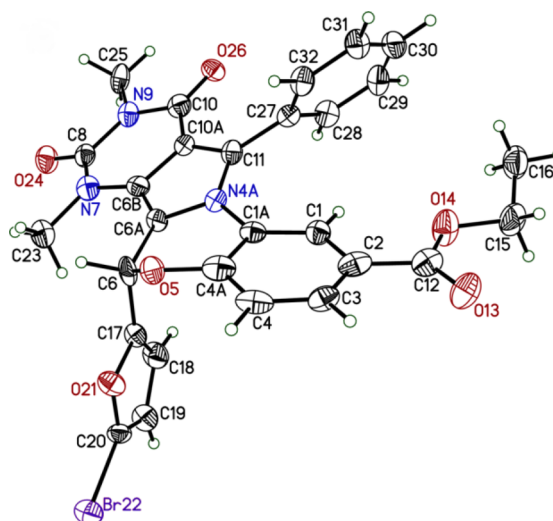
also argues against racemization, as racemic **3** would strongly inhibit CFTR at 100 nM. The chiral integrity of $(-)$-**2** was further confirmed by a hydrogen−deuterium exchange experiment. $(-)$-**2** was incubated under relevant physiological conditions in the presence of deuterium oxide. No reduction was found in the integrated signal of the singlet peak corresponding to the proton on the chiral carbon (see Supporting Information).

The in vitro metabolic stability of (R)-**1** and (S)-**1** was determined using rat hepatic microsomes. Following compound incubation with hepatic microsomes in the presence of NADPH, the nonmetabolized compound was quantified by LC/MS. Figure 4A shows little metabolism of either enantiomer.
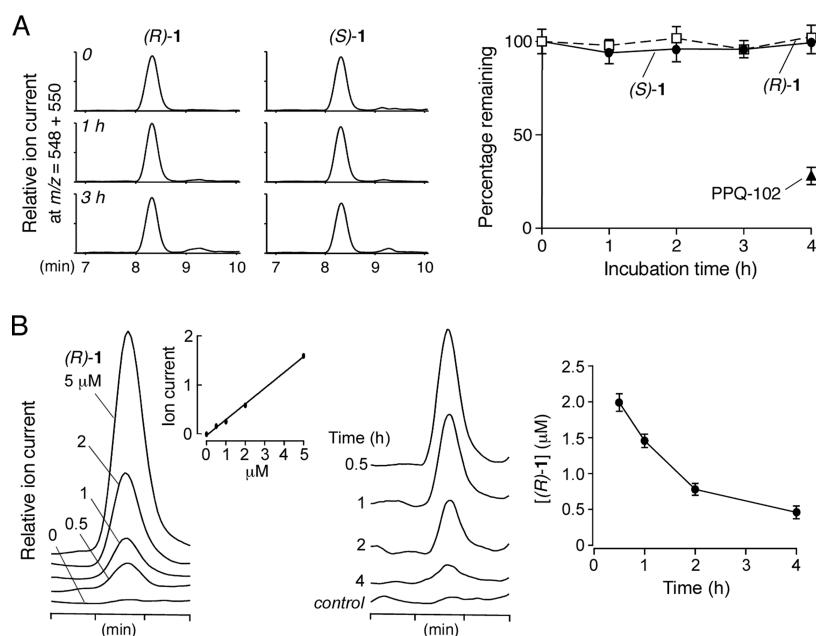
Figure 4. Metabolic stability of compound **1**. (A) In vitro metabolic stability of **1** measured in rat hepatic microsomes supplemented with NADPH. (left) LC/MS chromatograms of nonmetabolized enatiomers of **1** at indicated times. (right) Percentage nonmetabolized **1** remaining (S.E., $n = 4$). (B) In vivo pharmacokinetics of (R)-**1** in mice following bolus intraperitoneal injection at 10 mg/kg body weight. (left) Reference measurement. LC/MS chromatograms in which known amounts of (R)-**1** were added to blood and then extracted. Inset shows assay linearity. (right) LC/MS chromatograms of blood at indicated times after bolus intraperitoneal injection. (R)-**1** ion chromatograms ($m/z = 548 \, [M + H]^+$) are shown along with summary of serum concentration data (mean $\pm$ S.E., $n = 3$).

The pharmacokinetics of (R)-**1** was measured in mice by bolus intraperitoneal administration in an aqueous formulation consisting of 5% DMSO, 2.5% Tween-80, and 2.5% PEG400 in water. The concentration of (R)-**1** was measured by LC/MS in the blood and kidney. Figure 4B (left) shows ion current in calibration studies in which specified amounts of (R)-**1** were added to mouse blood. The assay was linear with a detection sensitivity of better than 500 nM (R)-**1**. Figure 4B (right) shows serum (R)-**1** concentration following bolus intra-peritoneal administration. The $t_{1/2}$ for the disappearance of the original compound was ~1.6 h. (R)-**1** concentration remained at predicted therapeutic levels ($\gg$IC$_{50}$ of 4 nM) for many hours following single dose administration. Using a CFTR inhibition bioassay to distinguish between active (R)-**1** and inactive (S)-**1**, we confirmed no measurable interconver-sion of the enantiomers in serum at 4 h. LC/MS analysis of kidney homogenate at 4 h showed a concentration of 0.6 ± 0.3 μM (3 mice).

In summary, chiral chromatography separated $(\pm)$-**1** into nearly pure enantiomers, one of which was ~2-fold more potent at inhibiting the CFTR chloride current than the racemic mixture, while the other enantiomer was inactive. The absolute configuration of the active enantiomer is R as determined by X-ray crystallography. The target of (R)-**1** and its analogues is likely CFTR itself, as these compounds inhibit CFTR chloride current in response to different types of agonists, including activators that target CFTR directly.[15,16] Definitive determination of the (R)-**1** binding site will require mutagenesis, molecular modeling, and/or biochemical studies.

■ ASSOCIATED CONTENT

Ⓢ Supporting Information

Detailed description of chromatography parameters, chemical synthesis, bioassay procedures, crystallographic information, and NMR. This material is available free of charge via the Internet at http://pubs.acs.org.

■ AUTHOR INFORMATION

Corresponding Author

*(A.S.V.) Tel: 415-476-8530. Fax: 415-665-3847. E-mail: alan. verkman@ucsf.edu. Webpage: http://www.ucsf.edu/verklab.

Author Contributions

All authors contributed to writing of this manuscript and approved the final version.

Notes

The authors declare no competing financial interest.

■ ABBREVIATIONS

ADPKD, autosomal dominant polycystic kidney disease; BPO, benzopyrimido-pyrrolo-oxazinedione; CFTR, cystic fibrosis transmembrane conductance regulator; DMAP, dimethylami-nopyrdine; EDC, 1-ethyl-3-(3-dimethylamino-propyl)-carbodiimide HCl; EtOAc, ethyl acetate; EtOH, ethanol; PKD, polycystic kidney disease; PPQ, pyrimido-pyrrolo-quinoxaline-dione; SiO$_2$, silica gel; SFC, supercritical fluid chromatography; TLC, thin layer chromatography

■ REFERENCES

(1) Riordan, J. R. CFTR function and prospects for therapy. *Annu. Rev. Biochem.* **2008**, 77, 701−726.

(2) Thiagarajah, J. R.; Verkman, A. S. CFTR pharmacology and its role in intestinal fluid secretion. *Curr. Opin. Pharmacol.* **2003**, *3*, 594−599.

(3) Venkatasubramanian, J.; Ao, M.; Rao, M. C. Ion transport in the small intestine. *Curr. Opin. Gastroenterol.* **2010**, *26*, 123−128.

(4) Torres, V. E.; Harris, P. C.; Pirson, Y. Autosomal dominant polycystic kidney disease. *Lancet* **2007**, *369*, 1287−1301.

(5) Yang, B.; Sonawane, N. D.; Zhao, D.; Somlo, S.; Verkman, A. S. Small-molecule CFTR inhibitors slow cyst growth in polycystic kidney disease. *J. Am. Soc. Nephrol.* **2008**, *19*, 1300−1310.

(6) Verkman, A. S.; Galietta, L. J. Chloride channels as drug targets. *Nat. Rev. Drug Discovery* **2009**, *8*, 153−171.

(7) Ma, T.; Thiagarajah, J. R.; Yang, H.; Sonawane, N. D.; Folli, C.; Galietta, L. J.; Verkman, A. S. Thiazolidinone CFTR inhibitor identified by high-throughput screening blocks cholera toxin-induced intestinal fluid secretion. *J. Clin. Invest.* **2002**, *110*, 1651−1658.

(8) Thiagarajah, J. R.; Song, Y.; Haggie, P. M.; Verkman, A. S. A small molecule CFTR inhibitor produces cystic fibrosis-like submucosal gland fluid secretions in normal airways. *FASEB J.* **2004**, *18*, 875−877.

(9) Sonawane, N. D.; Muanprasat, C.; Nagatani, R., Jr.; Song, Y.; Verkman, A. S. In vivo pharmacology and antidiarrheal efficacy of a thiazolidinone CFTR inhibitor in rodents. *J. Pharm. Sci.* **2005**, *94*, 134−143.

(10) Muanprasat, C.; Sonawane, N. D.; Salinas, D.; Taddei, A.; Galietta, L. J.; Verkman, A. S. Discovery of glycine hydrazide pore-occluding CFTR inhibitors: mechanism, structure−activity analysis, and in vivo efficacy. *J. Gen. Physiol.* **2004**, *124*, 125−137.

(11) Sonawane, N. D.; Hu, J.; Muanprasat, C.; Verkman, A. S. Luminally active, nonabsorbable CFTR inhibitors as potential therapy to reduce intestinal fluid loss in cholera. *FASEB J.* **2006**, *20*, 130−132.

(12) Sonawane, N. D.; Zhao, D.; Zegarra-Moran, O.; Galietta, L. J.; Verkman, A. S. Lectin conjugates as potent, nonabsorbable CFTR inhibitors for reducing intestinal fluid secretion in cholera. *Gastroenterology* **2007**, *132*, 1234−1244.

(13) Sonawane, N. D.; Verkman, A. S. Thiazolidinone CFTR inhibitors with improved water solubility identified by structure−activity analysis. *Bioorg. Med. Chem.* **2008**, *16*, 8187−8195.

(14) Sonawane, N. D.; Zhao, D.; Zegarra-Moran, O.; Galietta, L. J.; Verkman, A. S. Nanomolar CFTR inhibition by pore-occluding divalent polyethylene glycol-malonic acid hydrazides. *Chem. Biol.* **2008**, *15*, 718−728.

(15) Tradtrantip, L.; Sonawane, N. D.; Namkung, W.; Verkman, A. S. Nanomolar potency pyrimido-pyrrolo-quinoxalinedione CFTR inhibitor reduces cyst size in a polycystic kidney disease model. *J. Med. Chem.* **2009**, *52*, 6447−6455.

(16) Snyder, D. S.; Tradtrantip, L.; Yao, C.; Kurth, M. J.; Verkman, A. S. Potent, metabolically stable benzopyrimido-pyrrolo-oxazine-dione (BPO) CFTR inhibitors for polycystic kidney disease. *J. Med. Chem.* **2011**, *54*, 5468−5477.